URN (Paper): urn:nbn:de:gbv:ilm1-2014iwk-017:0

58th ILMENAU SCIENTIFIC COLLOQUIUM
Technische Universität Ilmenau, 08 – 12 September
2014 URN: urn:nbn:de:gbv:ilm1-2014iwk:3

COMPLIANT SHEAR FORCE SENSOR

Chaykina Alexandra, Griebel Stefan, Zentner Lena

Technische Universität Ilmenau, Mechanism Technology Group

ABSTRACT

This paper presents a novel compliant sensor for detecting the magnitude and direction of applied shear force or distribution of shear forces on a surface. The operating principle of the sensor is based on the large deformation capacity of silicone elastomers. The magnitude of the shear force is determined by measuring the internal pressure in the moment of electrical contact closing or opening. The sensor is particularly suitable for human-machine interfaces, such as robotics and medical technology.
The functionality of the proposed shape is tested using the finite elements method (FEM). Subsequently, the sensor is constructed and the selected principle for detecting the magnitude and direction of shear force is verified by metrological test.

Index Terms – shear force, compliant sensor, silicone elastomer, internal pressure, electrical contact

1. INTRODUCTION

Sensors for the determination of shear forces are used especially in robotics and medical technology. For example, information about the shear forces acting between an object and a robot gripper is required to realize a safe gripping in robotics [1,2].
For medical applications, the determination of shear forces is also often necessary. The early detection of the shear forces occurring at the contact points between the support system and the patient minimizes the risk of pressure ulcers developing [3]. The determination of shear forces is required for the development of orthopedic shoes, to study the physiology of the foot and for the prevention of injuries [4,5]. Also, in prosthetics, determination of the shear force could be envisaged as enabling better adaptation of the prosthesis [6].
One of the most important requirements for the sensors used at the human-machine interface, particularly in medical applications is a certain degree of compliance. Sensors for the detection of shear forces, known from the state of the art, usually consist of four sub-components: sensor elements for energy conversion (for example, piezoelectric [4], [7], piezoresistive [6], [8,9], capacitive [10,11] optical [12,13], inductive or magnetoresistive [14] sensor elements), of devices for transmitting the force to the sensor elements (force transmitting mechanisms), and of data lines with evaluation electronics.
The shear force sensors can be divided into rigid and compliant sensors depending on the material of the sensor elements and the force transmitting mechanisms. Most of the known solutions are not completely compliant. In such cases, the lack of compliance is addressed by embedding the sensor elements and force transmitting mechanisms in a flexible substrate [6], [8,9]. This embedding process leads to additional costs, because the highly elastic materials have to be bonded with low elastic materials. Furthermore, a completely compliant version is

preferable for reasons of minimizing the injury risks and comfort at the human-machine interface.
This paper describes a completely compliant sensor for shear force determination. The sensor makes it possible to detect in a simple way the magnitude and direction of applied shear force or distribution of shear forces on a surface.

2. MATERIAL AND METHODS

Silicone elastomers are suitable as the basic material for the sensor. These materials are commercially available in different Shore hardnesses. Due to the contained fillers such as carbon black, the conductive silicone elastomers can change their specific resistance if extended or compressed [15]. They thus have an effect which can be used for the sensor development. Also, such elastomers can be used as electrical conductors. This enables simple principle solutions for the development of a compliant sensor.

2.1 Operating Principle

Fig. 1 shows the sensor design. The sensor consists of one elastic touch element, one elastic deformation element and four electrodes. All of these are positioned on a base plate. The elastic touch element is connected to the deformation element and to the base plate in an airtight manner and forms a cavity. Via an air supply, it is possible to change the compressed air p_i in the cavity. Four electrodes are arranged concentrically around the deformation element. The electrodes allow a displacement in the z-direction, whereby the distance a_E between the touch element and the electrodes is adjustable.

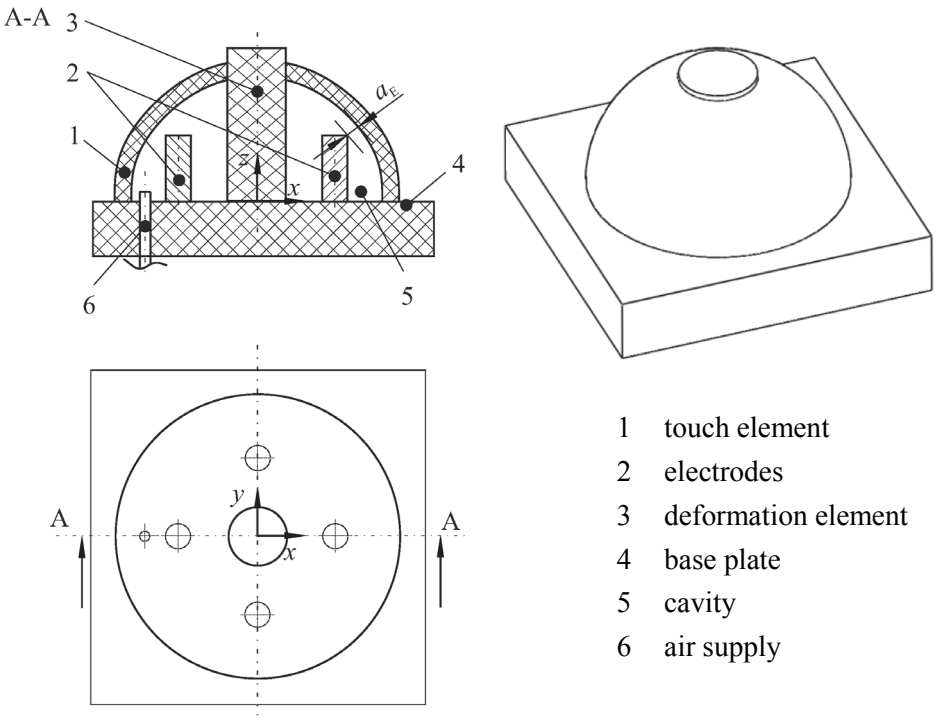

Fig. 1. Sensor design

The deformation element and the base plate are made of non-conductive material; the touch element and the electrodes, however, are made of conductive material.
The operating principle of the sensor is depicted in Fig. 2. If a shear force $\vec{F}_{Shear}$ is applied, the deformation element will be distorted. This results in a change of distance a_E between the

touch element and the corresponding electrode. There is a minimum force F^*_{Shear} from which these two elements contact each other and, thus, close the electrical circuit. The distance a_{E} is also dependent on the internal pressure p_{i}. Hence, this minimum force F^*_{Shear} is also dependent on the internal pressure p_{i}. This allows us to determine the magnitude of the shear force F_{Shear} by measuring the internal pressure p_{i} at the moment when the electrical contact closes or opens. For this reason, a supply voltage U_{s} is applied between the touch element and the electrode (see Fig. 2a).

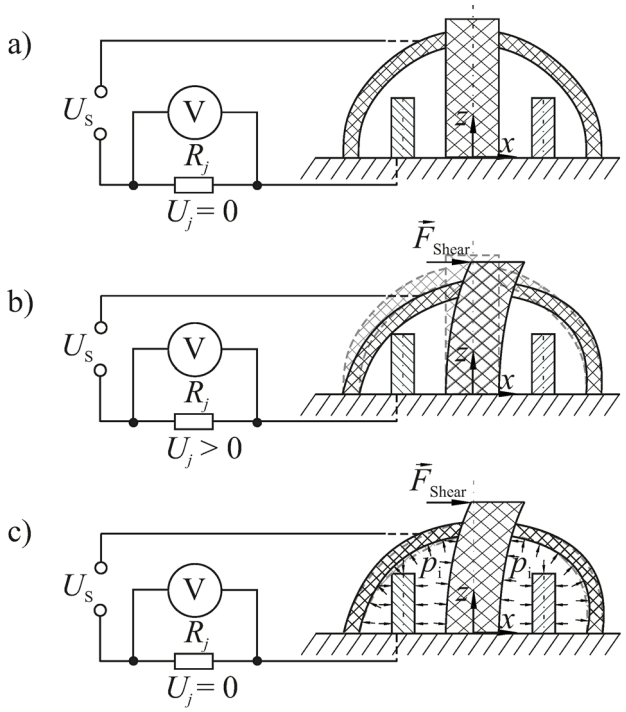

Fig. 2. Schematic representation of the operating principle: a) sensor in the initial state; b) sensor under the influence of shear force $\vec{F}_{\mathrm{Shear}}$; c) sensor under the influence of shear force $\vec{F}_{\mathrm{Shear}}$ and of internal pressure p_{i}

The closing of the electrical contact can be detected, for example, by identifying the voltages U_j across the resistors R_j (where j is the number of electrodes). If a shear force $\vec{F}_{\mathrm{Shear}}$ is applied and the contact is closed, a non-zero voltage U_j will be detected across the resistor R_j (see Fig. 2b). If the internal pressure p_{i} increases, the contact will be opened and the voltage takes the value 0 V (see Fig. 2c).

The sensor is also capable of detecting the direction of a shear force. Fig. 3a shows a plan view of the sensor (see Fig. 1) without electrical connections in the initial state.

If a shear force $\vec{F}_{\mathrm{Shear}}$ is applied to the deformation element, the contact will be closed depending on the direction of the shear force and its magnitude between at least one, and a maximum of two electrodes with the inner wall of the touch element. A non-zero voltage U_j (where $j = 1\ldots4$ is the number of electrodes) can subsequently be detected across the corresponding resistors R_j. Furthermore, in all other circuits without contact the voltage U_j is equal to 0 V. If the internal pressure p_{i} increases, the closed contacts will be opened again. The internal pressures $p_{\mathrm{i},j}$ have to be measured at the moment the contact opens. The measurement of the shear force magnitude is therefore at the moment the contact opens. In the diagrams, this is indicated by an arrow and the abbreviation CO (Contact Opening).

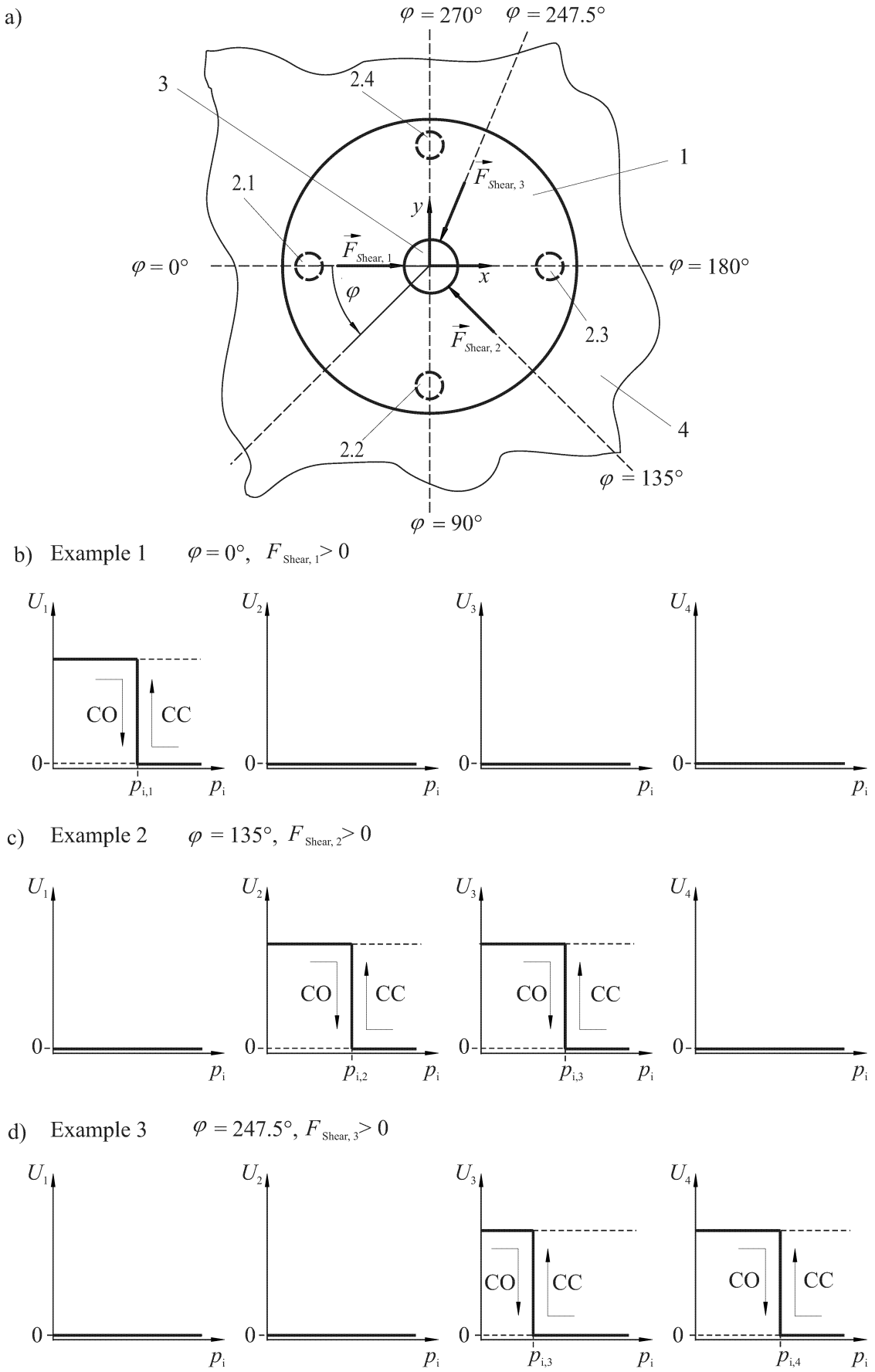

Fig. 3. Principle of direction recognition: a) plan view of sensor; b) – d) diagrams of voltage change of four electrodes for different shear force directions

The individual contributions of the shear force are then determined using the sensor characteristic curves $F^*_{\mathrm{Shear},j}(p_\mathrm{i})$ of the respective electrode. The resultant shear force is calculated according to equation (1):

$$\vec{F}^*_{\mathrm{Shear,\,res}} = \left(F^*_{\mathrm{Shear,\,1}}\left(p_{\mathrm{i},1}\right) - F^*_{\mathrm{Shear,\,3}}\left(p_{\mathrm{i},3}\right)\right)\vec{e}_x + \left(F^*_{\mathrm{Shear,\,2}}\left(p_{\mathrm{i},2}\right) - F^*_{\mathrm{Shear,\,4}}\left(p_{\mathrm{i},4}\right)\right)\vec{e}_y \qquad (1)$$

In this case, by means of the electrode 2.1 ($j = 1$) and pressure $p_{\mathrm{i},1}$, the magnitude of the shear force component $F^*_{\mathrm{Shear,\,1}}(p_{\mathrm{i},1})$ in the positive x-direction is determined. The magnitude of the shear force component $F^*_{\mathrm{Shear,\,2}}(p_{\mathrm{i},2})$ in the positive y-direction is determined via the electrode 2.2 ($j = 2$) and $p_{\mathrm{i},2}$. The magnitudes of the shear force components $F^*_{\mathrm{Shear,\,3}}(p_{\mathrm{i},3})$ in the negative x-direction and $F^*_{\mathrm{Shear,\,4}}(p_{\mathrm{i},4})$ in the negative y-direction are measured accordingly via the electrode 2.3 ($j = 3$) and $p_{\mathrm{i},3}$ and via the electrode 2.4 ($j = 4$) and $p_{\mathrm{i},4}$.

Example 1 (Fig. 3b): If a shear force $\vec{F}_{\mathrm{Shear},1}$ acts in the direction $\varphi = 0°$ (see Fig. 3a), it comes to the closing of the contact of the inner wall of the touch element with the electrode 2.1. A change in the voltage U_1 can be detected. The circuits of the electrodes 2.2, 2.3 and 2.4 are not closed. The corresponding voltages U_2, U_3 and U_4 are equal to 0 V. By increasing the internal pressure p_i (according to the arrow with abbreviation CO), the contact to the electrode 2.1 will be opened at the pressure $p_{\mathrm{i},1}$. Then, the magnitude of the shear force F^*_{Shear} can be determined using the sensor characteristic curve $F^*_{\mathrm{Shear,\,1}}(p_\mathrm{i})$.

Example 2 (Fig. 3c): If a shear force $\vec{F}_{\mathrm{Shear},2}$ acts in the direction $\varphi = 135°$ (see Fig. 3a), it comes to the closing of the contact of the inner wall of the touch element with the electrode 2.2 and with the electrode 2.3. A change in the voltage U_2 and U_3 can be detected through these electrodes' closed circuits. The circuits of the electrodes 2.1 and 2.4 are not closed. The corresponding voltages U_1 and U_4 are equal to 0 V. It can therefore be concluded that the shear force acts from the 2nd quadrant ($\varphi = 90°$, $\varphi = 180°$). By increasing the internal pressure p_i (according to the arrow with abbreviation CO), the contact to the electrode 2.2 will be opened at the pressure $p_{\mathrm{i},2}$ and to the electrode 2.3 at the pressure $p_{\mathrm{i},3}$. The contribution of the shear force component in the positive y-direction $F^*_{\mathrm{Shear,\,2}}(p_{\mathrm{i},2})$ can then be determined using the sensor characteristic curve $F^*_{\mathrm{Shear,\,2}}(p_\mathrm{i})$. The contribution of the shear force component in the negative x-direction $F^*_{\mathrm{Shear,\,3}}(p_{\mathrm{i},3})$ is determined by means of the sensor characteristic curve $F^*_{\mathrm{Shear,\,3}}(p_\mathrm{i})$. Since the force acts from the direction $\varphi = 135°$, the calculated pressures at the same distance a_E are equal, $p_{\mathrm{i},2} = p_{\mathrm{i},3}$. Therefore, the magnitudes of the determined shear force components $F^*_{\mathrm{Shear,\,2}}(p_{\mathrm{i},2})$ and $F^*_{\mathrm{Shear,\,3}}(p_{\mathrm{i},3})$ are also equal. The magnitude and direction of the shear force can be determined by vectorial addition of the two components with equation (1). The angle φ is calculated from equation (2).

$$\varphi = \left(1 - \Phi\left(F^*_{\mathrm{Shear,1}}\left(p_{\mathrm{i},1}\right)\right)\right)\cdot\pi + \arctan\left(\frac{\left(F^*_{\mathrm{Shear,2}}\left(p_{\mathrm{i},2}\right) - F^*_{\mathrm{Shear,4}}\left(p_{\mathrm{i},4}\right)\right)}{\left(F^*_{\mathrm{Shear,1}}\left(p_{\mathrm{i},1}\right) - F^*_{\mathrm{Shear,3}}\left(p_{\mathrm{i},3}\right)\right)}\right) \qquad (2)$$

with the Heaviside function according to equation (3):

$$\Phi\left(F^*_{\mathrm{Shear,1}}\left(p_{\mathrm{i},1}\right)\right) = \begin{cases} 1, & \text{if } F^*_{\mathrm{Shear,1}}\left(p_{\mathrm{i},1}\right) \geq 0 \\ 0, & \text{if } F^*_{\mathrm{Shear,1}}\left(p_{\mathrm{i},1}\right) < 0 \end{cases} \qquad (3)$$

Example 3 (Fig. 3d): It is also possible to measure the shear force by means of the closing of the contact. For this, the internal pressure p_i should be chosen to be so high that while, for example, a shear force $\vec{F}_{Shear,\,3}$ is acting in the direction $\varphi = 247.5°$, no contact is closed. The voltages to be measured U_1 to U_4 are then equal to zero. If the internal pressure p_i is slowly released to $p_i = 0$ (according to the arrow with abbreviation CC), it comes to a contact closing (CC) of the touch element with the electrode 2.3 at pressure $p_{i,3}$ and with the electrode 2.4 at pressure $p_{i,4}$. Thus, a non-zero voltage U_3 and U_4 can be detected through the electrodes' closed circuits. The circuits of electrodes 2.2 and 2.1 are not closed at the end of the measurement at the internal pressure $p_i = 0$. The corresponding voltages U_1 and U_2 are equal to zero throughout the measurement time. In conclusion, the shear force acts from the 3rd quadrant ($\varphi = 180°$, $\varphi = 270°$). The contribution of the shear force component in the negative x-direction $F^*_{Shear,\,3}(p_{i,3})$ can then be determined using the sensor characteristic curve $F^*_{Shear,\,3}(p_i)$ and the contribution of the shear force component in the negative y-direction $F^*_{Shear,\,4}(p_{i,4})$ can be determined using the sensor characteristic curve $F^*_{Shear,\,4}(p_i)$. Since the force acts from the direction $\varphi = 247.5$, the calculated pressures are not equal at the same distance a_E. In this case, the pressure $p_{i,4}$ is greater than $p_{i,3}$. Therefore, the magnitudes of the determined shear force components $F^*_{Shear,\,3}(p_{i,3})$ and $F^*_{Shear,\,4}(p_{i,4})$ are different. The magnitude and direction of the shear force can be determined by vectorial addition of the two components with equation (1). The angle φ is calculated from equations (2) and (3).

2.2 FEM Analysis

Since, the operating principle of the sensor is based on a large deformability, and highly elastic materials with a non-linear stress-strain curve are used, the proposed geometry was investigated using the finite elements method (FEM) and the ANSYS Workbench program. The aim of the simulations was to determine the minimum shear force F^*_{Shear} from which the touch element and the corresponding electrode contact each other for different pressures p_i. Thereby, the closing of the electrical contact was interpreted by a mechanical contact in the model. Fig. 4 shows a side view of the FEM model with the geometric parameters.

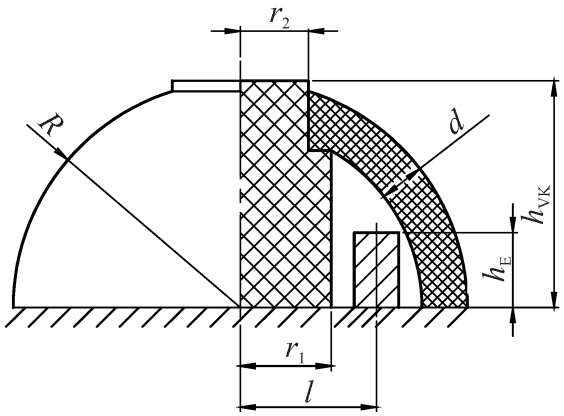

Fig. 4. FEM model: $R = 20$ mm, $r_1 = 4$ mm, $r_2 = 3$ mm, $l = 6$ mm, $d = 2$ mm, $h_E = 3{,}5$ mm, $h_{VK} = 10$ mm

The FEM model consists of three elements: a deformation element, a touch element and an electrode. The elements are mounted on a fixed bearing in the model. The contact points between the touch element and the electrode are defined as frictionless.

To represent the behavior of the functional model as accurately as possible, uniaxial tensile tests for the silicone elastomers Elastosil® 420/30 (non-conductive) and Elastosil® 570/50

(conductive) were carried out in the run-up to the simulation. These two silicone elastomers were chosen as materials for the manufacturing of a later functional model. The measured data were fitted by the non-linear material model Ogden 3rd Order. Furthermore, the material model for Elastosil® 420/30 was assigned to the deformation element and the material model for Elastosil® 570/50 to the touch element. Structural steel was chosen as the material for the electrode. The simulation was divided into two load steps. During the first load step, the internal pressure p_i was increased. This pressure p_i acted on all internal surfaces of the sensor body. During the second load step, the shear force $\vec{F}_{Shear}$ was applied. Nine simulation series were carried out for the maximum pressure from 0 to 0.04 MPa in 0.005 MPa increments. The maximum shear force $F_{Shear,max}$ was 7 N for all simulations. In order to determine the shear force F^*_{Shear} through simulations, the second load step was divided into 20 sub steps. While increasing the shear force in discrete steps from 0 N to 7 N, it comes above a certain value of force to contact between the touch element and the electrode. Thereby, a portion of the shear force is transferred onto the electrode (see Fig. 5).

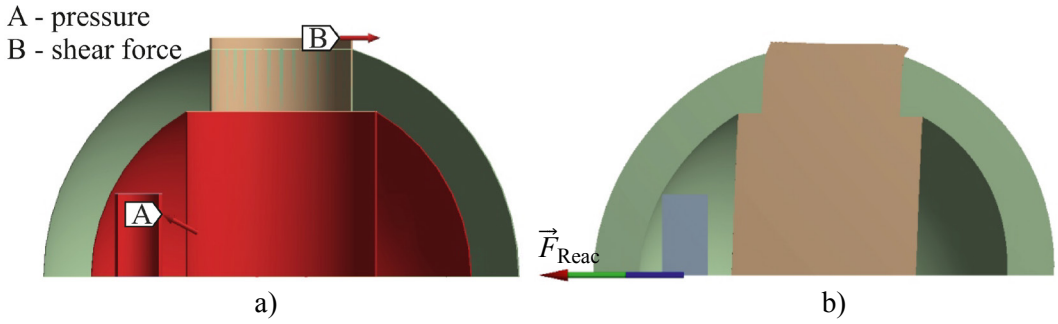

Fig. 5. Simulation model: a) the initial state with the loads; b) the deformed state with the reaction force $\vec{F}_{Reac}$ on the electrode base

This means that the closing of the contact and thus the value of the shear force F^*_{Shear} can be detected using the reaction force $\vec{F}_{Reac}$ on the electrode base.

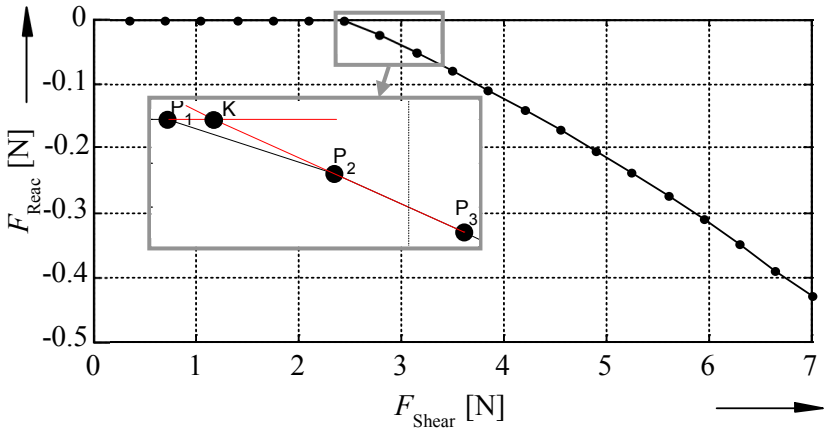

Fig. 6. The change of the reaction force $\vec{F}_{Reac}$ as a function of the shear force $\vec{F}_{Shear}$

Fig. 6 shows the change of the reaction force $\vec{F}_{Reac}$ as a function of the shear force $\vec{F}_{Shear}$ for an internal pressure p_i of 0 MPa. In order to find the shear force F^*_{Shear}, a straight line was put through the next two points P_2 and P_3 so that this line intersects the zero axis. The intersection point K corresponds to the shear force $F^*_{Shear}=F_{Shear}|_K$, which leads to the contact (see Fig. 6). A necessary condition is: $F^*_{Shear}>F_{Shear}|_{P_1}$.

From nine simulation series, nine points of the shear force F^*_{Shear} belonging to the sensor characteristic curve $F^*_{\mathrm{Shear}}(p_\mathrm{i})$ were determined. Fig. 7 shows the points determined, which are approximated by a straight line.

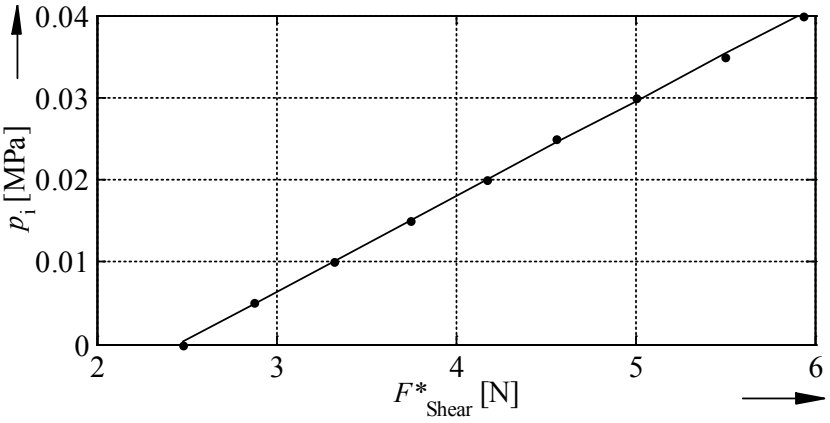

Fig. 7. Points F^*_{Shear} approximated by a straight line

The approximation error does not exceed 1.2%. Therefore, the approximation line is assumed to be a sensor characteristic curve of the proposed sensor.

3. EVIDENCE OF FUNCTIONALITY

In order to provide evidence of functionality, a functional model was built and investigated through a metrological test. For manufacturing reasons, not all components of the functional model were made of highly elastic materials. Further, completely compliant single sensors can be manufactured and built in a matrix. Thus, sensor surfaces of any size can be created to determine the distribution of shear forces on a surface.

3.1 Functional Model Fabrication

For the manufacture of the deformation element and touch element, which consist of silicone, two molding tools were designed and manufactured.

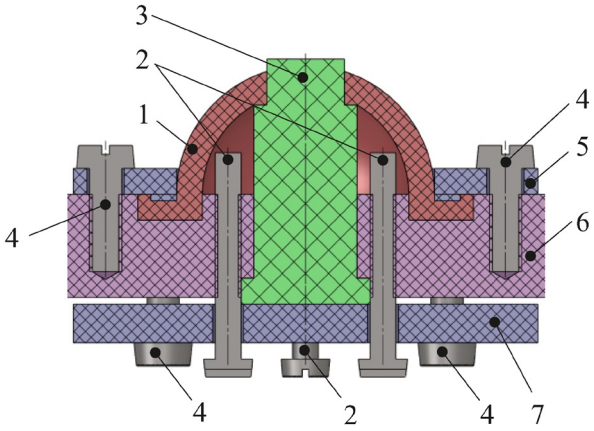

1 touch element
2 electrodes = screws
3 deformation element
4 fixing screws
5 upper fixing ring
6 plastic plate
7 lower fixing ring

Fig. 8. Functional model

The silicone parts produced were mounted on a plastic plate. Fig. 8 illustrates the built sensor in cross-section. The operating principle of the sensor requires an airtight connection of the individual elements. This is achieved in the functional model by screwing and gluing the

individual components together. The necessary air tightness is ensured by the interlocking of the components and the elasticity of the silicone. The electrodes are simple screws here. In addition, the plastic plate has a through hole under the cavity area of the touch element (not shown in the figure). This hole is used as an air supply for the compressed air.

3.2 Metrological Tests

In order to determine the minimum shear force F^*_{Shear} from which the touch element and the corresponding electrode close the contact for different pressures p_i, metrological tests were carried out. The shear force was provided to the functional model by a material testing machine (ProLine table-top testing machine Z005) equipped with a measurement and control computer. For this purpose, an aluminum plate having a bore with a diameter of 6 mm at the end was clamped in the jaws of the material testing machine. The sensor was positioned so that the deformation element lay in the bore of the aluminum plate up to the connection point with the touch element (see Fig. 9). The tests were performed at the normal force equal to 0 N.

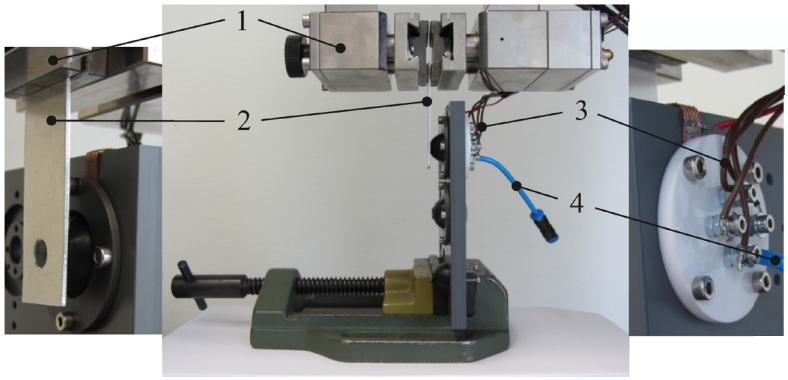

1 jaws of testing machine
2 aluminum plate
3 electrical conductors
4 air connection

Fig. 9. Test setup of the sensor tilted into a vertical position: a) front view; b) side view; c) back view

Through the air supply the sensor was impinged with a pressure p_i. The closing of the contact between the touch element and the electrode was detected by the voltage detection between these two elements. The deformation element was displaced by 3 mm at a velocity of 3 mm/min. Simultaneously, the resulting force and voltage were determined.

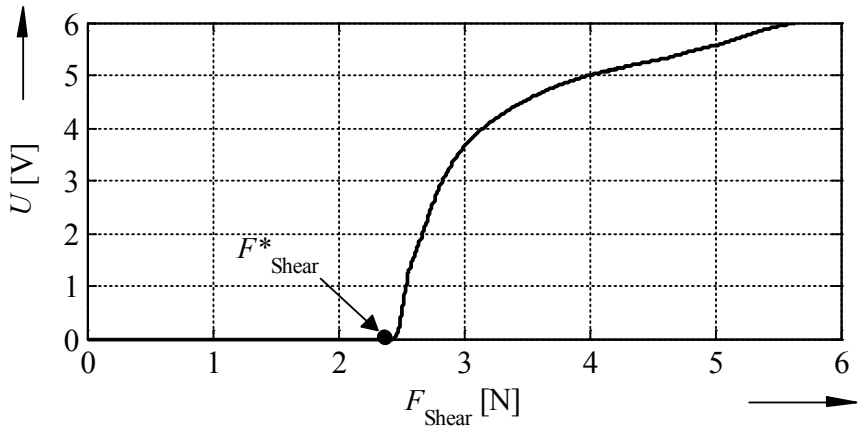

Fig. 10. Determination of the shear force F^*_{Shear}

Fig. 10 shows the determination of the shear force F^*_{Shear} by the change in the voltage as a function of the shear force $\vec{F}_{Shear}$ for the internal pressure $p_i = 0$ MPa.
Metrological tests were carried out for the maximum pressure from 0 to 0.04 MPa in 0.005 MPa increments.

3.3 Results

From the metrological tests, the points of the shear force F^*_{Shear} were determined for different internal pressures p_i. Then, these points were approximated by a straight line. The maximum approximation error was less than 1.5%. The points determined during the simulation and metrological tests were compared with each other (see Fig. 11). Here, the maximum relative error between the points is 3.1%.

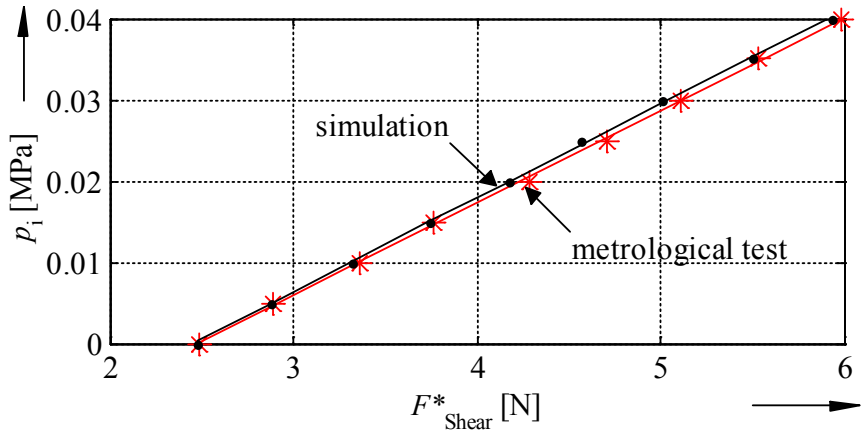

Fig. 11. The points of the shear force F^*_{Shear} for the simulation and metrological tests approximated by a straight line

The tests carried out showed that the shear forces can be determined by the proposed sensor system in the range from 2.5 N to 6 N. For this, the internal pressures p_i have to be varied from 0 to 0.04 MPa. The influence of the normal force on the sensor characteristic was not considered.

4. SUMMARY AND OUTLOOK

The compliant shear force sensor was developed. The sensor is simple, made of highly elastic materials and has a nearly linear characteristics curve. This represents a great potential for human-machine interfaces, such as medical applications and robotics.
It is evident that the influence of normal forces would change the characteristics curve of the sensor. Further work is therefore required to investigate this influence.

5. ACKNOWLEDGMENT

The authors would like to thank the Thuringian State Graduate Support for financial support.

REFERENCES

[1] K. Noda et al., “A shear stress sensor for tactile sensing with the piezoresistive cantilever standing in elastic material”, Sensors and Actuators A 127, pp. 295–301, 2006

[2] D. Yamada et al., “Artificial finger skin having ridges and distributed tactile sensors used for grasp force control”, In: IEEE International Conference on Intelligent Robots and Systems, pp. 686–691, 2001

[3] P. Diesing, „Prüf- und Bewertungsmethoden für Antidekubitus-Systeme“, Dissertation, Technical University of Berlin, 2006

[4] S. Kärki et al., “Development of a piezoelectric polymer film sensor for plantar normal and shear stress measurements”, Sensors and Actuators A 154, pp. 57–64, 2009

[5] E. Heywood et al., “Tri-axial plantar pressure sensor: design, calibration and characterization”, In: Annual International Conference of the IEEE EMBS, pp. 2010–2013, 2004

[6] L. Beccai, et al., “Design and fabrication of a hybrid silicon three-axial force sensor for biomechanical applications”, Sensors and Actuators A 120, pp. 370–382, 2005

[7] J. Dargahi, “A piezoelectric tactile sensor with three sensing elements for robotic, endoscopic and prosthetic applications”, Sensors and Actuators 80, pp. 23–30, 2000

[8] K. Kim, “A silicon-based flexible tactile sensor for ubiquitous robot companion applications”, Journal of Physics: Conference Series 34, pp. 399–403, 2006

[9] G. Vasarhelyi et al., “Characterization of an integrable single-crystalline 3-D tactile sensor”, Sensors Journal, IEEE, 4, pp. 928–934, 2006

[10] H.-K. Lee et al., “Real-time measurement of the three-axis contact force distribution using a flexible capacitive polymer tactile sensor”, Journal of Micromechanics and Microengineering 21, pp. 1-9, 2011

[11] J. Novak et al., “Initial Design and Analysis of a Capacitive Sensor for Shear and Normal Force Measurement”. In: Proceedings of IEEE International Conference on Robotics and Automation, pp. 137-144, 1989

[12] M. Ohka et al., “Sensing Precision of an Optical Three-axis Tactile Sensor for a Robotic Finger”, In: The 15th IEEE International Symposium on Robot and Human Interactive Communication, pp. 214–219, 2006

[13] W.-C. Wang et al., “A shear and plantar pressure sensor based on fiber-optic bend loss”, The Journal of Rehabilitation Research and Development 3, pp. 315–326, 2005

[14] M. Lord, R. Hosein, R. B. Williams, “Method for in-shoe shear stress measurement”, Journal of Biomedical Engineering 14 (3), pp. 181–186, 1992

[15] H.J. Mair, S. Roth, „Elektrisch leitende Kunststoffe“, 2. vollständig überarbeitete und erweiterte Auflage, Carl Hanser Verlag, Munich, Vienna, 1989

CONTACTS

Dipl.-Ing. A. Chaykina alexandra.chaykina@tu-ilmenau.de
Dipl.-Ing. S. Griebel stefan.griebel@tu-ilmenau.de
Prof. Dr.-Ing. habil. L. Zentner lena.zentner@tu-ilmenau.de